Multilayer Neural Network-Burg Combination for Acoustical Detection of Buried Objects

Mujahid AL-Azzo[1] and Lubna Badri[2]
[1]Faculty of Engineering Technology, Zarqa Private University, Jordan
[2]Faculty of Engineering, Philadelphia University, Jordan

Abstract: *A Burg technique is employed to model the long wavelength localization and imaging problem. A Burg method is used as a high resolution and stable technique. The idea of in-line holography is used to increase the ratio of the signal to noise due to the effect of concealing media that decreases the value of the received signal. The performance is enhanced by using multilayer neural network for noise reduction. The aim of using multilayer neural network is to extract the essential knowledge from a noisy training data. Theoretical and experimental results have showed that preprocessing the noisy data with multilayer neural network will decrease the effect of noise as much as possible. Applying the enhanced data to spectral estimation methods has improved the performance of the model. A comparison is made for the two cases: with and without application of neural network for different values of signal to noise ratio. Also, the performance is investigated for different numbers of samples.*

Keywords: *Multilayer neural networks, holographic imaging, burg method, and modelling.*

Received November 13, 2008; accepted August 3, 2009

1. Introduction

Neural network techniques for noise reduction have been investigated [1, 2, 4, 6, 7, 12, 14], and the main design goal of these neural networks was to get a good approximation for some input-output mapping. In addition to obtaining a conventional approximation, neural networks are expected to generalize from the given training data. The generalization is to use information that NN learned during training period in order to synthesize, similar but not identical, input-output mapping [14]. In this paper, a Multilayer Neural Network (MLNN) have been designed, trained, and tested. During training, the input sequences are presented to the network, and there outputs are calculated and compared with the target sequences (desired signals) to generate an error sequences. The input training sequences are assumed to be a composition of the desired signal plus an additive white Gaussian noise. For each time step, the error is back propagated to find the gradients of errors. This gradient is then used to update the weights. The network is expected to learn the noisy training data with the corresponding desired output and generalize the model.

The long wavelength radiation has applied to imaging and detection [9] since it is a highly coherent waves. The interest in ultrasound waves [11] stems from its property as the ability to penetrate many media that are optically opaque. This makes them very important for detecting and imaging targets that cannot be imaged by light waves. The in-line holography is employed, where the reflected wave from the object under imaging is added at the receiver to a reference wave. The resulting wave (signal) is known as hologram. The in-line holography, with digital image reconstruction can be a simple and economic imaging technique using FFT method [16]. The ultrasonic hologram is recorded by mechanical scanning of a transmit/receive transducers over its aperture. The use of holography enables improvement of the signal-to-noise ratio by coherently cumulating the acoustic field on the ultrasonic transducers when scanning the field [15].

The nonparametric power spectrum estimation approaches are relatively simple, and easy to compute via the FFT algorithm. However, these methods require the availability of long data records in order to yield the necessary frequency resolution; here resolution means the minimum separation between two points of the object that can be distinguished. Furthermore, these methods suffer from spectra leakage effects due to windowing that is inherent in finite- length data records [13]. Therefore it is required to use other technique that can enhance the resolution. A Burg method contributes itself as a high resolution and stable method [3, 13].

2. Multilayer Neural Network

The aim is to train back propagation neural network (a multilayer feed forward network trained by back

propagation) to achieve a balance between the ability to respond correctly to the input patterns that are used for training (memorization) and the ability to give reasonable responses to input that is similar, but not identical, to that used in training (generalization). Variations of back propagation training algorithms have been developed to improve the speed and performance of the training process.

2.1. Architecture

A MLNN is designed with three layers as shown in Figure 4. The feed forward network has two hidden layers of tansig neurons (*f1* and *f2*) followed by an output layer of purelin neurons (*f3*). The numbers of neurons in the first and second hidden layers are 7 and 3, respectively. The hidden units and the output unit also have biases. These bias terms act like weights on connections from units whose output is always 1. Multiple layers of neurons with nonlinear transfer functions allow the network to learn nonlinear and linear relationship between input and output vectors.

The elements of the weight vector w are ordered by layer (starting from the first hidden layer), then by neurons in a layer, and then by the number of a synapse within a neuron. Let *Wji(l)* denote the synaptic weight from neuron *i* to neuron *j* in layer l. For l=1, corresponds to the first hidden layer, the index *i* refers to a source node rather than a neuron, as shown in Figure 1. Only the direction of information flow for the feed forward phase of operation is shown. During the back propagation phase of learning, signals are sent in the reverse direction.

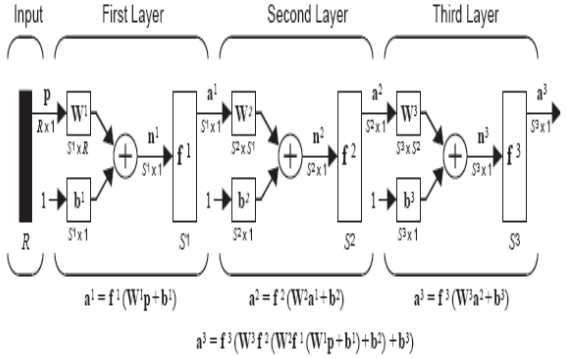

Figure 1. The architecture of three-layer neural network [10].

2.2. Learning with Back Propagation Algorithm

What makes this algorithm different than the others is the process by which the weights are calculated during the learning phase of the network. The difficulty with multilayer Perceptron is calculating the weights of the hidden layers in an efficient way that results in the least output error; the more hidden layers there are, the more difficult it becomes.

A number of network architectures have been designed and tested with different noisy data samples. The aim was to have efficient training process, to avoid overtraining problem, and to have better Mean Square Error (MSE). The research results indicate that for the given model, with a reasonable number of training samples, a network with two hidden layers was sufficient to achieve the required aims.

It has been proven [4] that the addition of random noise to the desired signal during the training process of the neural network can improve the generalization of the network and can avoid the learning process from being trapped into local minimum.

Assume x_k denotes the k^{th} element of an input vector; y_i is the ith output of the output layer. Let $d_i(t)$ denote the desired response for output neuron i at time *t*, where t is the discrete time index.

The error signal $e_i(t)$ is defined as the difference between the target response $d_i(t)$ and the actual response $y_i(t)$.

$$e_i(t) = d_i(t) - y_i(t) \tag{1}$$

The aim of learning is to minimize a cost function based on the error signal $e_i(t)$, with respect to network parameters (weights), such that the actual response of each output neuron in the network approaches the target response [4].

A criterion commonly used for the cost function is the MSE criterion, defined as the mean-square value of the sum squared error:

$$J = E\left[\frac{1}{2}\sum_i \left(e_i(t)\right)^2\right] \tag{2}$$

$$= E\left[\frac{1}{2}\sum_i \left(d_i(t) - y_i(t)\right)^2\right] \tag{3}$$

where *E* is the statistical expectation operator and the summation is over all the neurons of the output layer. Usually the adaptation of weights is performed by using the desired signal $d_i(t)$ only.

In [4] it is stated that a new signal $d_i(t) + n_i(t)$ can be used as a desired signal for output neuron i instead of using the original desired signal $d_i(t)$, where $n_i(t)$ is a noise term. This noise term is assumed to be white Gaussian noise, independent of both the input signals $x_k(t)$ and the desired signals $d_i(t)$. With the new desired signals, the MSE of equation 3 can be written as:

$$J = E\left[\frac{1}{2}\sum_i \left(d_i(t) + n_i(t) - y_i(t)\right)^2\right] \tag{4}$$

It is shown in [1] that equation 4 is equal to:

$$J = \frac{1}{2}E\left[\sum_i \left(y_i(t) - E\{d_i(t) + n_i(t) \mid x(t)\}\right)^2\right] + \frac{1}{2}E\left[\sum_i \mathrm{var}\left(\left(d_i(t) + n_i(t)\right) \mid x(t)\right)\right] \tag{5}$$

where the symbol $\mid$ means conditional probabilities and 'var' is an abbreviation of variance. The second term in the right hand side of equation 5 will contribute to the total error *J* and as learning progresses, but it does not affect the final value of the weights because it

is not a function of the network weights, while the first term will decide the optimal value of the weights [4]. Since the noise is zero mean and it is independent of both desired and the input signals, thus:

$$\{\mathrm{E}\{d_i(t) + n_i(t)|x(t)\} = \{\mathrm{E}\{d_i(t)|x(t)\} \quad (6)$$

It is clear from equations 5 and 6 that the final weight values can be determined without the existence of noise in the equation.

3. Holographic Imaging

3.1. Field Analysis

Holography is an interference technique for recording the amplitude and phase of a coherent wave, whether it is electromagnetic or acoustic. A recording of this interference pattern is called a hologram.

For simplicity, we start the analysis of the field at the receiving (hologram) plane. The object, under imaging process, is assumed to have field distribution *D(p)*. The distribution is caused by reflecting the incident ultrasonic waves on the object. This distribution propagates to the recording axis *X* where it produces the field distribution *S(x),* given by:

$$S(x) = \frac{B}{Z_o \lambda} \int_p D(p) \exp(\, jkr(p,x)dp \quad (7)$$

This is the paraxial approximation to the Huygens-Fresnel principles [8]. B is a complex constant, k is a propagation constant(wave number), Zo is the distance between the object and recording(observation) planes, and r is the distance from a typical point on the object to a typical point on the recording axis X. r is given as :

$$r(p,x) = \sqrt{Z_o^2 + (x-p)^2} \quad (8)$$

According to paraxial approximation, where

$$((x-p)^2 / Z_o^2) \langle\langle 1 \quad (9)$$

Then equation 8 is written as:

$$r(p,x) = Z_o + \frac{(x-p)^2}{2Z_o} - \frac{(x-p)^4}{8Z_o^3} + ---- \quad (10)$$

In Fresnel region, r can be approximated by the first two terms of equation 10, hence

$$r(p,x) = Z_o + \frac{x^2}{2Z_o} + \frac{p^2}{2Z_o} - \frac{px}{Z} \quad (11)$$

Substituting equations 11 and 7 yields

$$S(x) = B_1 \exp(\frac{jkx^2}{2Z_o}) \int_p D(p) \exp(\frac{jkp^2}{2Z_o}) \exp(\frac{-jkxp}{Z_o}) dp \quad (12)$$

where, *B1* is a complex constant resulting from equations 7 and 11.

3.2. Analysis of In-Line Hologram

Figure 2 shows the geometry of recording the in-line hologram with a plane-wave reference. This type of wave can be easily synthesized in an experimental recording system by simply introducing a constant reference signal in the receiver.

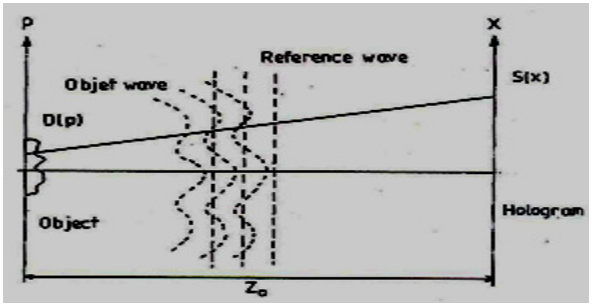

Figure 2. Hologram recording geometry.

Assuming that the synthesized plane-wave reference is $A_r \exp(j\Phi)$ where A_r and Φ are constants. The in-line hologram *h(x)* is given by [8].

$$\begin{aligned} h(x) &= |S(x) + A_r \exp(j\phi)|^2 \\ &= A_r^2 + |S(x)|^2 + A_r \exp(j\phi) S^*(x) + A_r \exp(-j\phi) S(x) \end{aligned} \quad (13)$$

An image can be extracted from the recorded hologram *h(x)* through its multiplication by either one of the focusing phase factors $exp(\frac{\mp jkx^2}{2z_0})$ and subsequent Fourier transformation [16] (a classical method) or one of the modern high resolution spectral analysis, like Burg, method. A positive phase factor produces an in-focus image from the third term of *h(x)* and defocused image from its fourth term while the negative phase factor achieves the opposite result. For both signs of the phase factor, the second term produces a defocused autocorrelation function of *D(p)* and the first term generate a Fresnel diffraction pattern related to the hologram boundary. Thus, while only one term of *h(x)* produces an in-focus image, the other three terms generate interference that obscure the wanted image. It has been shown [16] that the effect of these interfering terms can be considerably reduced. The first term A_r^2 is constant and can be subtracted from the recorded hologram prior to reconstruction [15, 16].

The training of MLNN was made to follow the model described by the following equation:

$$d(x) = A_r^2 + S^2 + 2A_r S\mathrm{Cos}\,\theta \quad (14)$$

where θ is a phase difference between A_r and S. This is equivalent to equation 13.

4. Burg Algorithm

The Burg method [13] for estimating the AutoRegressive (AR) parameters can be viewed as an order – recursive least-squares lattice method , based on the minimization of the forward and backward errors in linear predictors, with the constraint that the *AR* parameters satisfy the Levinson-Durbin recursion. To derive the estimator, suppose that we are given the data *S(n)*, *n=0,1,..., N-1*, and let us consider the forward and backward linear prediction estimates of order *m*, given as [13]

$$\hat{S}(n) = -\sum_{k=1}^{m} a_m(k) S(n-k) \tag{15}$$

$$\hat{S}(n-m) = -\sum_{k=1}^{m} a_m^*(k) S(n+k-m) \tag{16}$$

and the corresponding forward and backward errors $f_m(n)$ and $g_m(n)$ defined as

$$f_m(n) = S(n) - \hat{S}(n) \text{ and}$$

$$g_m(n) = S(n-m) - \hat{S}(n-m)$$

where $a_m(k)$, $0 \le k \le m-1$, *m=1,2,...,p*, are the prediction coefficients, and p is the AR process order. The least square error is

$$\varepsilon_m = \sum_{n=m}^{N-1} \left[\left| f_m(n) \right|^2 + \left| g_m(n) \right|^2 \right] \tag{17}$$

This error is to be minimized by selecting the prediction coefficients, subject to the constraint that the Levinson-Durbin recursion given by [13]

$$a_m(k) = a_{m-1}(k) + K_m a_{m-1}^*(m-k) \qquad \begin{matrix} 1 \le k \le m-1 \\ 1 \le m \le p \end{matrix} \tag{18}$$

where $K_m = a_m(m)$ is the m^{th} reflection coefficient in the lattice filter realization of the predictor. When equation 18 is substituted into the expressions for $f_m(n)$ and $g_m(n)$, the result is the pair of order –recursive equations for the forward and backward prediction errors given by [13]

$$\begin{aligned} f_m(n) &= f_m\text{-}1(n) + k_m g_{m-1}(n-1), \quad m = 1,2,....,p \\ g_m(n) &= K_m^* f_{m-1}(n) + g_{m-1}(n-1), \quad m = 1,2,....,p \end{aligned} \tag{19}$$

Now, using equations 18 and 19 and performing the minimization of ε_m with respect to the complex – valued reflection coefficient K_m, we obtain the result [13].

$$\hat{K}_m = \frac{-\sum_{n=m}^{N-1} f_{m-1}(n) g_{m-1}^*(n-1)}{\frac{1}{2} \sum_{n=m}^{N-1} \left[\left| f_{m-1}(n) \right|^2 + \left| g_{m-1}(n-1) \right|^2 \right]} \quad \text{m=1,2,...p} \tag{20}$$

The term in the numerator of equation 20 is an estimate of the cross correlation between the forward and backward prediction errors. With the normalization factors in the denominator of equation 20, it is apparent that $|K_m| < 1$, so that the all-pole model obtained from the data is stable. The denominator in equation 20 is simply the least-squares estimate of the forward and backward errors E_{m-1}^f and E_{m-1}^b, respectively [13]. Hence equation 20 can be expressed as

$$\hat{K}_m = \frac{-\sum_{n=m}^{N-1} f_{m-1}(n) g_{m-1}^*(n-1)}{\frac{1}{2} \left[\hat{E}_{m-1}^f + \hat{E}_{m-1}^b \right]} \quad \text{m=1,2,...,p} \tag{21}$$

where $\hat{E}_{m-1}^f + \hat{E}_{m-1}^b$ is an estimate of the total squared error E_m. The denominator term of equation 21 can be computed in an order-recursive fashion according to the relation [13]

$$\hat{E}_m = \left(1 - \left| \hat{K}_m \right|^2 \right) \hat{E}_{m-1} \left| f_{m-1}(m-1) \right|^2 - \left| g_{m-1}(m-2) \right|^2 \tag{22}$$

where $\hat{E}_m \equiv \hat{E}_m^f + \hat{E}_m^b$ is the total squared error [13]. To summarize, the Burg algorithm computes the reflection coefficients in the equivalent lattice structure as specified by equations 21 and 22, and the Levinson-Durbin algorithm is used to obtain the AR model parameters. From the estimate of the AR parameters, the power spectrum estimate is formed as [13]

$$P_{xx}^{BU}(f) = \frac{\hat{E}_p}{\left| 1 + \sum_{k=1}^{p} \hat{a}_p(k) e^{-j2\pi fk} \right|^2} \tag{23}$$

The major advantages of the Burg method for estimating the parameters of the AR model are equation 1 it results in high frequency resolution [3, 13], equation 2 it yields a stable AR model [3, 13], and equation 3 it is computationally efficient.

5. Experimental Results

In this paper, a test object consisting of two steel rods of 2.5cm diameter was used. The separation between the two rods was 7.5cm. The object was located at a distance Z_o cm from the recording (hologram) plane. The object was concealed (covered) by opaque materials, a sheet of paper and a Styrofoam in two separate experiments. The object was illuminated by ultrasound waves using ultrasonic transmitting transducers.

The received signals from the object due to the reflection are recorded and in order to enhance them, or in other words, to decrease the effect the environments such as the relatively high background that caused by the concealing material; a MLNN is

designed and used as a preprocessing technique for noise reduction.

In order to develop the designed neural network performance, it must be well trained using many training sets and different training algorithms. The training sets are extracted from the desired model plus different added random noise. Neural network tool box in Matlab software provides many training back propagation functions. These functions are used during the learning process of the neural network to continuously updating the weights and biases of the system to incrementally reduce the error between the desired model and the neural network actual output. The MSE is used as a performance goal to indicate the end of the training process.

Table1. Multilayer Neural Network Performance with two experiments cases: sheet of paper and styrofoam isolating materials.

Training Algorithm	Mean Square Error (MSE)	
	Sheet of Paper Case	Styrofoam Case
Traingd	0.053542	0.177533
Traingdm	0.014463	0.170649
Traingda	0.0157362	0.15886
Trainlm	0.0112285	0.149683
Traingdx	0.0126875	0.164845

Table 1 shows the results obtained after training the network with different back propagation functions. All of these algorithms use the gradient of the performance function to determine how to adjust the weights to minimize the error between the desired model and the actual NN output. These algorithms are Traingd, Traingdm, Traingda, Trainlm, and Traingdx [10]. It is clear from the results obtained Table 1 that Trainlm back propagation function results in a fastest algorithm implementation (90 epochs) with a best performance (MSE equals 0.0112285) in comparison with other functions. The Trainlm function works according to Levenberg-Marquardz optimization technique [10]. Figure 3 shows the neural network performance during the training process with tarinlm back propagation algorithm. The designed neural network is able to decrease the effect of concealing medium and noisy captured signal.

After training the MLNN on different input patterns, the network was ready to accept the measured input signals. It is worthwhile to mention that, the resolution formula for FT method is given as [16].

$$\beta = \frac{\lambda Z_o}{b} \tag{24}$$

where 2*b* is the hologram length.

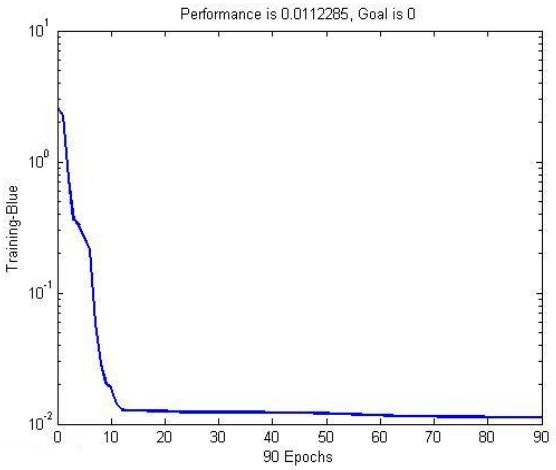

Figure 3. Multilayer neural network performance during the training process.

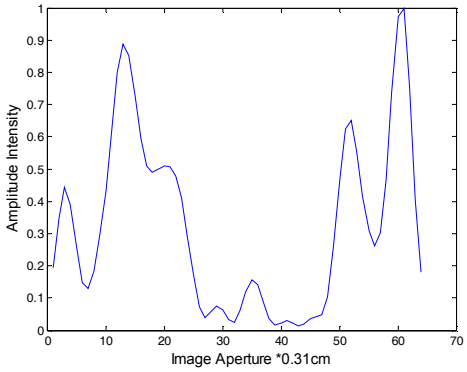

Figure 4. Reconstructed image of two rods using FT method, the concealing material is a sheet of paper.

Figure 4 shows the reconstructed image when FFT method was used. The highest two peaks are corresponding to the two rods. Practically, the minimum number of samples, *N*, was 20, to resolve the two rods. This represents about three times the minimum number of samples required by equation 24 to resolve the two peaks. Also the effect of sidelobes and the degrading effect of the concealing material are noticeable. When Burg method was used, the two peaks that belong to the two rods are well defined, the sidelobes are very small or negligible and the effect of the concealing plate is very little as shown in Figure 5. Hence the Burg method detects clearly the target parameter: the amplitude of the reflected signal which is received at hologram.

In order to study the problem more deeply, using Burg method, and to compare the performance between the two cases, with and without using the MLNN, a white noise was added to the hologram and its effect on the results has been investigated. The absolute difference between the amplitude of the two peaks, in dB, is regarded as an amplitude error, because, theoretically, it is expected that the received signals from the two rods are of the same values since the two rods are similar.

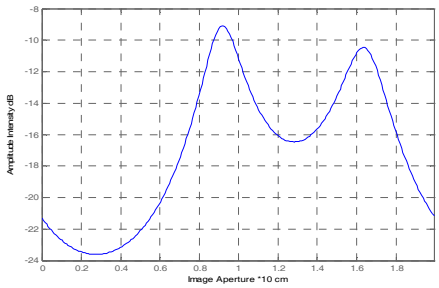

Figure 5. Reconstructed image of two rods with Burg method and without using multilayer NN. The concealing material is a sheet of paper.

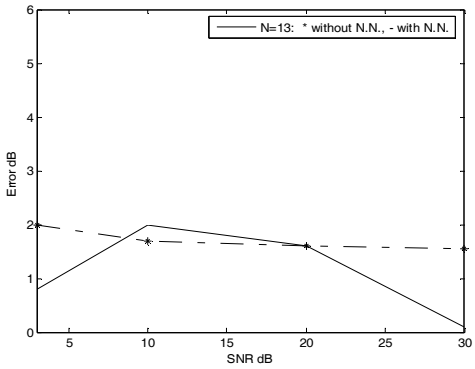

Figure 6. Error in absolute difference between peaks (amplitude) as a function of signal to noise ratio _sheet of paper.

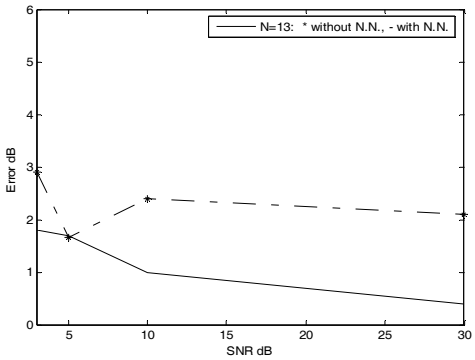

Figure 7. Error in absolute difference between peaks (amplitude) as a function of signal to noise ratio (Styrofoam).

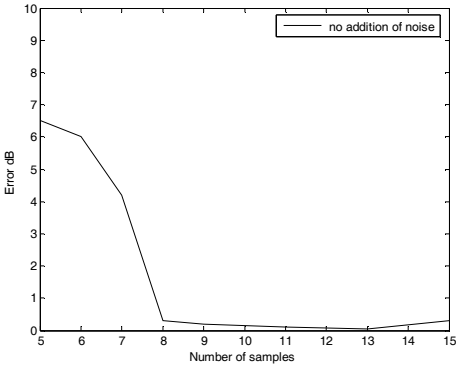

Figure 8. Error in absolute difference between the two peaks (amplitude) as a function of number of samples (sheet of paper).

Figures 6 and 7 show the performance with and without using the neural network on the resultant error as a function of Signal-To-Noise (SNR) ratio for both concealing materials. It is clear that as the SNR decreases, the performance degrades. The degradation is not so severe when SNR decreases to about 0 dB. This is because the addition of a reference wave, in recoding the in-line hologram, will result in a coherently cumulating the acoustic field on the ultrasonic transducers when scanning the field. The implementation of MLNN improves more the performance, and hence decreases the effect of the concealing plate.

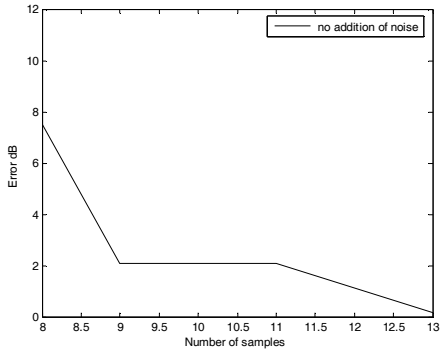

Figure 9. Error in absolute difference between the two peaks (amplitude) as a function of number of samples (Styrofoam).

When *N* decreased, similar results were obtained to clearly define the two peaks. The performance of the neural network-Burg method is studied by varying the number of samples. Figures 8 and 9 show the amplitude error as a function of the number of samples for both concealing materials. The performance breakpoint, for the case of sheet of paper, is when *N=7*, while it is equal to 8 for the case of Styrofoam.

6. Conclusions

In this research, a number of MLNN architecture have been studied and tested to obtain the optimal architecture in terms of number of hidden layers and neurons in each layer. The results obtained show that during the pre-processing stage, the MLNN was able to enhance the tested recorded signal and produce an output signal that follows the desired model with very good performance. It is demonstrated that the Burg method can be used to detect and image a concealed object of closely separated points. Experimental results show that pre-processing the noisy data with MLNN to decrease the effect of noise as much as possible and then applying the enhanced data to spectral estimation method can improve the performance. Also the use of holography enables an improvement of the signal-to-noise ratio by coherently cumulating the acoustic field on the ultrasonic transducers when scanning the field.

References

[1] Badri L. and Al-Azzo M., "Modelling of Long Wavelength Detection of Objects Using Elman Network Modified Covariance Combination," *International Arab Journal of Information*

Technology (IAJIT), vol. 5, no. 3, pp. 265-272, 2008.

[2] Bakker B., "The State of Mind Reinforcement Learning with Recurrent Neural Networks," *PhD Thesis*, Leiden University, 2004.

[3] Bos R., de Waele S., and Broersen T., "Autoregressive Spectral Estimation by Application of the Burg Algorithm to Irregularly Sampled Data," *Computer Journal of IEEE Transactions on Instrumentation and Measurement*, vol. 51, no. 6, pp. 1989-1994, 2002.

[4] Chuan W. and Jose P., "Training Neural Networks with Additive Noise in the Desired Signal," *Computer Journal of Transation on Neural Networks*, vol. 10, no. 6, pp. 1511-1517, 1999.

[5] Demuth H. and Beale M., *Neral Network Toolbox: for Use with MATLAB*, The MathWorks, 2002.

[6] Dorronsoro J., López V., Cruz S., and Sigüenza A., "Autoassociative Neural Networks and Noise Filtering," *Computer Journal of IEEE Transactions on Signal Processing*, vol. 51, no. 3, pp. 1431-1438, 2003.

[7] Fred C. and Tony M., "Improved Hopfield Nets by Training with Noisy Data," *in Proceedings of of the IEEE International Joint Conference on Neural Networks*, UK, pp. 1138-1143, 2001.

[8] Goodman W., *Introduction to Fourier Optics*, Roberts Company Publisher, 2004.

[9] Gupta J., Beals J., and Moghaddar A., "Data Extrapolation for High Resolution Radar Imaging," *Computer Journal of IEEE Transactions on Antenna and Propagation*, vol. 42, no. 11, pp. 1540-1545, 1994.

[10] Hagan M., Demuth H., and Beale M., *Neural Network Design*, PWS Publishing Company and Thomson Asia Pre Ltd, 2002.

[11] Lee H. and Wade G., *Modern Acoustical Imaging*, NY IEEE Press, 1986.

[12] Parveen S. and Green P., "Speech Enhancement with Missing Data Techniques Using Recurrent Neural Networks," *in Proceedings of IEEE International Conference on Acoustics*, pp. I733-I736, 2004.

[13] Proakis J. and Manolakis D., *Digital Signal Processing: Principles, Algorithms and with Applications*, Prentice-Hall, 2007.

[14] Radonja P., "Neural Networks Based Model of a Highly Nonlinear Process," *IX Telekomunikacioni Forum Telfor'2001*, Beograd, 2001.

[15] Roux P., Casserau D., and Roux A., "A High Resolution Algorithm for Wave Number Estimation Using Holographic Array Processing," *Computer Journal of Acoustic Society of America*, vol. 115, no. 3, pp. 1059-1067, 2004.

[16] Sayidmarie H., Anderson P., and Bennet C., "Digital In-Line Holographic Techniques for Long Wavelength Imaging," *in Proceedings of IEE*, pp. 211-220,1982.

Mujahid Al-Azzo received the BSc, MSc, in electrical engineering /electronic and communication in 1982, and 1985, respectively, and the PhD in communication engineering in 1999, all from Mosul University/ Iraq. His interest is in the fields of signal processing, spectral analysis, and acoustical holographic imaging.

Lubna Badri received her BSc and MSc degree, in computer and control engineering, from the University of Technology, Baghdad in 1994 and 1996, respectively, and the PhD degree in computer engineering, from University of Technology in Baghdad, Iraq, in 1999. Her interest is in the fields of neural network and fuzzy logic, knowledge acquisition systems, and embedded system design.

.